

Photovoltaic effect in a periodically poled lithium niobate Solc-type wavelength filter

Lijun Chen,^{a)} Jianhong Shi, Xianfeng Chen,^{b)} and Yuxing Xia

Department of Physics, The State Key Laboratory on Fiber Optics Local Area Communication Networks and Advanced Optical Communication Systems, Shanghai Jiao Tong University, 800 Dongchuan Rd., Shanghai 200240, China

(Received 1 October 2005; accepted 21 February 2006; published online 23 March 2006)

We report a non-field-applied Solc-type filter constructed by a periodically poled lithium niobate (PPLN). By comparing two types of PPLN Solc filter setup, both theoretically and experimentally, we have proved that without external field applied, it is the photovoltaic effect that introduces pass peak in the PPLN band filter. © 2006 American Institute of Physics. [DOI: 10.1063/1.2187944]

With the maturity of the room temperature electric-poling technique,¹ periodically poled ferroelectric crystals, especially periodically poled lithium niobate, are being used in a variety of applications, such as harmonic generation, pulse compression, and soliton interaction. When the domain block inverses its spontaneous polarization direction, other parameters, such as electro-optic and photovoltaic coefficients, will also change their direction or sign. In our former research works,²⁻⁴ a Solc-type filter in PPLN is achieved, which has a narrow bandwidth and temperature-tunable pass-band wavelength. Furthermore, the output intensity of the filter can be controlled by the external electric field.

In the experiments, we also found that, without an external field, the device can also serve as a Solc filter, which has not been covered by any existing theory. In this letter, we suggest that the photovoltaic effect (PVE) plays an essential role in the performance of a non-field-applied PPLN Solc filter, which is substantiated by subsequent experiments.

Figure 1 shows a folded Solc-type filter.⁵ It contains a series of half-wave plates between two crossed polarizers, with the optic axes of the half-wave plates alternately aligned at the angles $+\theta$ and $-\theta$ with respect to an axis. This axis is always set to Z, and it is often parallel or normal to the polarization plane of the input polarizer.

The Jones matrix, a 2×2 -matrix method, is employed to track the polarization state of light propagation through the Solc filter. The transmissivity of the light wave after passing through the whole filter is given by

$$\begin{aligned} \begin{bmatrix} E'_z \\ E'_y \end{bmatrix} &= P_z M P_y \begin{bmatrix} E_z \\ E_y \end{bmatrix} \\ &= P_z \begin{bmatrix} M_{11} & M_{12} \\ M_{21} & M_{22} \end{bmatrix} P_y \begin{bmatrix} E_z \\ E_y \end{bmatrix} \quad \text{and} \quad T_A = |M_{12}|^2, \end{aligned} \quad (1)$$

where the input polarizer is set to Y, and the output polarizer is set to Z;

^{a)}Electronic mail: chain@sjtu.edu.cn
^{b)}Electronic mail: xfchen@sjtu.edu.cn

$$\begin{aligned} \begin{bmatrix} E'_z \\ E'_y \end{bmatrix} &= P_y M P_z \begin{bmatrix} E_z \\ E_y \end{bmatrix} \\ &= P_y \begin{bmatrix} M_{11} & M_{12} \\ M_{21} & M_{22} \end{bmatrix} P_z \begin{bmatrix} E_z \\ E_y \end{bmatrix} \quad \text{and} \quad T_B = |M_{21}|^2, \end{aligned} \quad (2)$$

where the input polarizer is set to Z, and the output polarizer one is set to Y. M is the Jones matrix of the whole series of plates (not including polarizers).

From the calculation of the matrix M , it yields⁵

$$M_{21} = \sin 4\theta \sin^2 \frac{1}{2}\Gamma \frac{\sin mK\Lambda}{\sin K\Lambda} = -M_{12},$$

$$K\Lambda = \cos^{-1} \left(\sin^2 2\theta \sin^2 \frac{1}{2}\Gamma + \cos^2 \frac{1}{2}\Gamma - \cos^2 2\theta \sin^2 \frac{1}{2}\Gamma \right), \quad (3)$$

where $\Gamma = 2\pi(n_o - n_e)(d/\lambda)$ is the phase difference of one half-wave plate, d is the plate thickness, m is the number of the plate couples, and $m = N/2$ (N is the number of all the plates). n_o and n_e are the refractive indices of the lithium niobate determined by the Sellmeier equation.^{6,7} Equations (1)–(3) indicate that the two types of crossed polarizers setups have the same transmission curve, i.e., $T_A = T_B$.

Figure 2 shows the relationship between the whole Solc filter transmissivity of power and its construction parameters

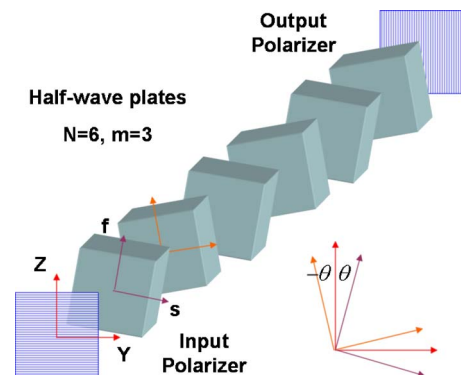


FIG. 1. (Color online) Folded Solc filter schematic diagram. m couples of half-wave plates are held in two crossed polarizers. The optic axes of the plates aligned at angles $+\theta$ and $-\theta$ with respect to the Z axis in every couple.

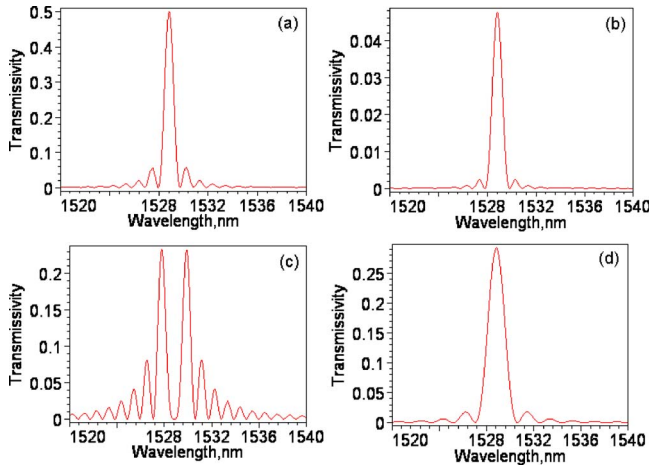


FIG. 2. (Color online) The theoretical power transmission curves of the PPLN Solc filter under various parameters at 24 °C, $d=10.4 \mu\text{m}$: (a) $m=1346$, $\theta=\pi/8m=\pi/10768$; (b) $m=1346$, $\theta=\pi/40m=\pi/53840$; (c) $m=1346$, $\theta=\pi/4m=\pi/5384$; (d) $m=746$, $\theta=\pi/8m=\pi/10768$.

θ, m, Γ , according to Eq. (3). The center pass wavelength is only determined by the phase delay of one plate, which is given by

$$\Gamma = (2\nu + 1)\pi, \quad \lambda_\nu = \frac{2}{2\nu + 1}(n_o - n_e)d, \quad \nu = 0, 1, 2, \dots, \quad (4)$$

where ν is the order of the filter passband or the order of the half-wave plate of one domain and is zero in this application. θ mainly determines the peak transmission value. When $\theta_f = \pi/8m$, the filter achieves the full pass peak, shown in Fig. 2(a). Because the input light is polarized, so the peak is 1/2 for the nature of the input light. When θ is smaller than the θ_f , the shape of the curve remains almost unchanged, but the peak value decreases [Fig. 2(b)]. However, θ cannot be set too large, otherwise the shape of the pass curve will be largely deformed [Fig. 2(c)]. m determines the peak width of the pass curve peaks as is shown in Fig. 2(d).

The Solc filter can be constructed with PPLN.^{8,9} In a lithium niobate crystal, due to the presence of an external electric field along the Y axis, the refractive index ellipsoid deforms, and consequently the Y and Z axes of the Z -cut lithium niobate rotate by a small angle θ about the X axis. Thus, in the presence of a uniform electric field along the Y axis, the rotation angle of the Y and Z axes changes sign from positive to negative from the noninverted domain to the inverted domain, correspondingly, in PPLN. With the placement of two crossed polarizers at the two ends of PPLN, a folded Solc-type filter is easily formed by applying a uniform electric field along the Y axis. If the field is along the Z axis, there is no θ induced. The only change is the refractive index, and no filter function exists.

When light propagates through the photorefractive crystal, PVE can lead to a uniform electric field as a result of the presence of photoinduced electric currents and voltages in the bulk dielectric material. The incident light will ionize impurities in the material, and these ionized charges will move in a particular direction inside the crystal without the presence of an external electric field. If the sample is uniformly illuminated and kept in open circuits, then a voltage between the faces can be observed. This current density can be described by the following linear equation:^{10,11}

$$\begin{bmatrix} J_1 \\ J_2 \\ J_3 \end{bmatrix} = \alpha \begin{bmatrix} 0 & 0 & 0 & 0 & G_{15} & -G_{22} \\ -G_{22} & G_{22} & 0 & G_{15} & 0 & 0 \\ G_{31} & G_{31} & G_{33} & 0 & 0 & 0 \end{bmatrix} \begin{bmatrix} E_1 E_1^* \\ E_2 E_2^* \\ E_3 E_3^* \\ E_1 E_2^* \\ E_1 E_3^* \\ E_2 E_3^* \end{bmatrix}, \quad (5)$$

where 1,2,3 correspond to the X, Y, Z axes of the Cartesian system, and the X axis is parallel to the a axis, and the Z axis is parallel to the c axis of the LiNbO₃ crystal with $3m$ symmetry. When a polarized light goes through the crystal, for different conditions we find the following.

When the light with Y polarized propagates in the X direction,

$$\begin{bmatrix} J_1 \\ J_2 \\ J_3 \end{bmatrix} = \alpha \begin{bmatrix} 0 \\ G_{22} \\ G_{31} \end{bmatrix} E_2 E_2^*. \quad (6)$$

When the light with Z polarized propagates in the X direction,

$$\begin{bmatrix} J_1 \\ J_2 \\ J_3 \end{bmatrix} = \alpha \begin{bmatrix} 0 \\ 0 \\ G_{33} \end{bmatrix} E_3 E_3^*. \quad (7)$$

The current is very small because of the small conductivity of the pure crystal. After several seconds, the current will lead to the accumulation of charges at the edge of the illuminated area, and thus establish a field that holds back the current. A balance can be accomplished as follows:¹²⁻¹⁴

$$\begin{aligned} J &= -\sigma E_{\text{sat}}, \\ \sigma &= \sigma_d + \sigma_{\text{ph}} I. \end{aligned} \quad (8)$$

σ is the conductivity of the lithium niobate that includes two parts: the dark conductivity σ_d and the photoconductivity σ_{ph} . E_{sat} is the saturation field in the bulk crystal that is established by PVE. I is the light intensity. From Eq. (5) to Eq. (8), at the Y direction, we obtain

$$E_{\text{sat } A} = -\alpha G_{22} E_2 E_2^* / \sigma \quad \text{for the situation of Eq. (6)}, \quad (9)$$

$$E_{\text{sat } B} = -\alpha 0 E_2 E_2^* / \sigma = 0 \quad \text{for the situation of Eq. (7)}. \quad (10)$$

Only the field E_{sat} in the Y direction can enable the Solc filter. If the input polarizer is put in the Y direction, there will be a field formed in the Y direction that will make the device work as a Solc filter; if the input polarizer is set in the Z direction, no field will cause the half-wave plate rocking. Then the PPLN will have no filter function and act just like a bulk crystal.

In the Solc filter, the polarization plane of the beam is not invariable and slowly changes its polarization. The Y direction field will decrease at the rear blocks of the PPLN, thus decreasing the pass peak of the filter. But it has no influence on the filter peak wavelength and main shape, which has been discussed in the filter parameter analysis before.

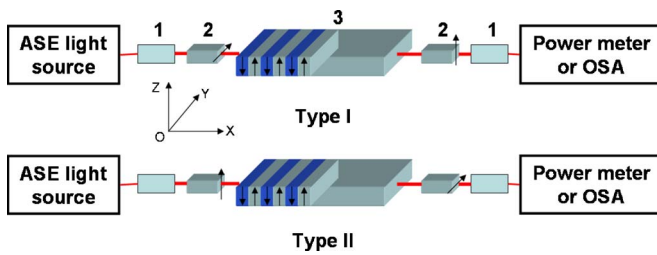


FIG. 3. (Color online) Two types of device setups for PPLN Solc-type wavelength filter; the arrow on the polarizer indicates the polarization direction. The fact that type A takes on the filter behavior while type B does not reveals the test light has the PVE on the PPLN and it becomes a Solc filter when no external field exists. The numbered components are: 1, collimator; 2, crossed polarizers; 3, PPLN.

Figure 3 shows the schematic diagram of the experiment. The filter is composed of a single chip PPLN crystal placed between two crossed polarizers. The PPLN is Z cut and light propagates along the X direction as indicated in the figure. There are two types of filter setups. In type A the input polarizer is set parallel to the Y direction, and the output polarization is parallel to the Z direction, thus perpendicular to the input polarizer. In type B the input polarization is set parallel to the Z direction, and the output polarization is parallel to the Y direction. The sample was 28 mm long, 5 mm wide, and 0.5 mm thick, which has a period of $20.8 \mu\text{m}$. The *c* axis of the PPLN is parallel to the Z axis.

In the test of the filter, an EXFO ASE light source with a total power of 9.3 mW is used. An optical spectrum analyzer (OSA) is used as the detector. The light is induced and exported by a couple of collimators with the insert loss about -2 dB . Since the filter center wavelength can be easily shifted by temperature, the data are measured at a constant temperature of about $20 \text{ }^\circ\text{C}$.

The results of the type A and type B filter pass curve are measured in Fig. 4. It shows that type A has a pass peak but type B has no obvious passband. In type A, the peak pass-

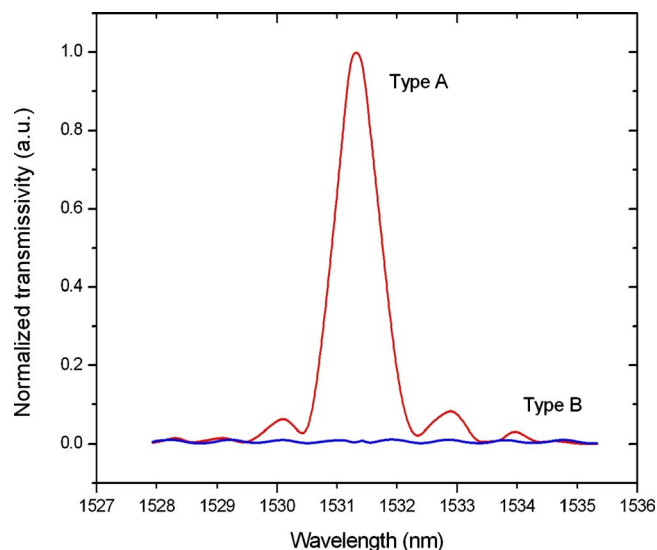


FIG. 4. (Color online) The transmission curve of the type A setup of device is in accord with the Solc filter function while the type B setup almost has no pass peak.

band centered in 1531.30 nm is 20 times higher in magnitude than the neighboring ripple. The center wavelength matches up with the theoretical prediction given by Eq. (4), and the transmission spectrum shows that it is a typical Solc-type wavelength filter. On the contrary, we do not find any wavelength filtering phenomenon in type B. We expect that there is a rocking angle in type A instead of in type B. This result is in good accord with our theoretical prediction as described above. We also found that there is a time span of several minutes for the type A filter performance to become stable. This slow procedure is characteristic of the PVE. We believe it is the PVE of the test light that is conducive to the field and causes the rocking angle of the Solc wavelength filter. When a voltage is applied along the Y direction, the rocking angle of the Solc filter is changed by the electrical field. As a result, the transmission of the filter is modulated by the applied field, which can be described by $T = \sin^2 2N\theta$, where θ is the total rocking angle induced by the PVE effect and also the applied voltage. In the case of type A, the electrical modulation behavior has been experimentally studied as shown in Fig. 3 in Ref. 2, in which a “phase shift” is observed. We attribute this phase difference of 0.991 rad to the PVE effect. On the contrary, in the case of type B, no phase difference is observed.

Both the theory and the experiment show that the PVEs play an important role in the formation of the Solc wavelength filter without an external applied field. The PVE effect sometimes cannot be neglected, especially in electric-optic devices. On the other hand, we can use this effect to build light controlled optical devices or to measure the PVE coefficients.

This research was supported by the National Science Foundation of China (Grant Nos. 60477016 and 10574092), the Foundation for Development of Science and Technology of Shanghai (04DZ14001) and the Excellent Young Teachers Program of MOE, People’s Republic of China.

¹M. Yamada, N. Nada, M. Saitoh, and K. Watanabe, *Appl. Phys. Lett.* **62**, 435 (1993).

²X. F. Chen, J. H. Shi, and Y. P. Chen, *Opt. Lett.* **28**, 2115 (2003).

³J. H. Shi, X. F. Chen, Y. P. Chen, Y. M. Zhu, Y. X. Xia, and Y. L. Chen, *Electron. Lett.* **39**, 224 (2003).

⁴Y. M. Zhu, X. F. Chen, and J. H. Shi, *Opt. Commun.* **228**, 139 (2003).

⁵A. Yariv and P. Yeh, *Optical Waves in Crystal: Propagation Control of Laser Radiation* (Wiley, New York, 1984).

⁶J. P. Meyn and M. M. Fejer, *Opt. Lett.* **22**, 1214 (1997).

⁷D. H. Jundt, *Opt. Lett.* **22**, 1553 (1997).

⁸Y. Q. Lu, Z. L. Wan, Q. Wang, Y. X. Xi, and N. B. Ming, *Appl. Phys. Lett.* **77**, 3719 (2000).

⁹D. R. Pinnow, R. L. Abrams, J. F. Lotspeich, D. M. Henderson, T. K. Plant, R. R. Stephens, and C. M. Walker, *Appl. Phys. Lett.* **34**, 391 (1979).

¹⁰L. Arizmendi, *Phys. Status Solidi B* **201**, 253 (2004).

¹¹B. I. Sturman and V. M. Fridkin, *The Photovoltaic and Photorefractive Effects in Noncentrosymmetric Materials* (Gordon and Breach, New York, 1992).

¹²E. Kratzig and H. Kurz, *Ferroelectrics* **13**, 295 (1976).

¹³M. Glass, D. von der Linde, and T. J. Negran, *Appl. Phys. Lett.* **25**, 233 (1974).

¹⁴M. Simon, St. Wevering, K. Buse, and E. Kratzig, *J. Phys. D* **30**, 144 (1997).